The Journal of Headache and Pain

RESEARCH

Open Access

Differentially localizing isoforms of the migraine component calcitonin gene-related peptide (CGRP), in the mouse trigeminal ganglion: βCGRP is translated but, unlike αCGRP, not sorted into axons

Sofia Lyng Wæver[1,2] and Kristian Agmund Haanes[1,2,3*]

Abstract

Objective The neuropeptide calcitonin gene-related peptide (CGRP) has been established to be a key signaling molecule in migraine, but little is known about the differences between the two isoforms: αCGRP and βCGRP. Previous studies have been hampered by their close similarity, making the development of specific antibodies nearly impossible. In this study we sought to test the hypothesis that αCGRP and βCGRP localize differently within the neurons of the mouse trigeminal ganglion (TG), using αCGRP knock out (KO) animals.

Methods We applied immunohistochemistry (IHC) on 15 TGs from three different genotypes of mice; wild type (WT) αCGRP heterozygote (Het) and αCGRP KOs, with a primary antibody targeting the mature neuropeptide sequence of both αCGRP and βCGRP. Subsequently, the localization patterns of the two isoforms were analyzed. Furthermore, similar IHCs were produced in KO animals after being treated with monoclonal CGRP antibodies to study the origin of the observed CGRP. Additional IHCs were conducted in KO and WT mice to locate CGRP sorting peptides within neuronal cell bodies. Lastly, bioinformatical analyses of the primary, secondary, and tertiary structure of the two isoforms were conducted.

Results The IHC showed that the key isoform localized within the axons of the mouse TG neurons, is αCGRP and not βCGRP. Furthermore, differences in intensities indicate that the model used in this study successfully knocks out αCGRP. We further categorized the localization patterns of CGRP in neuronal cell bodies in the TG and found using bioinformatic analyses that differences in localization might be explained by intracellular peptide sorting. IHC following injections with monoclonal CGRP antibodies in KO mice ruled out the possibility that the βCGRP observed in trigeminal neurons had peripheral origins. This conclusion was enhanced by IHC experiments which showed the presence of CGRP co-localizing sorting peptides in KO mice.

*Correspondence:
Kristian Agmund Haanes
khaa0039@regionh.dk

Full list of author information is available at the end of the article

Conclusion Our data show that mainly αCGRP and not βCGRP locate within the axons of the mouse TG neurons. The βCGRP observed within the TG neuronal cell bodies is synthesized intracellularly and not taken up from the environment. Furthermore, the isoforms appear to be sorted differentially into secretory vesicles in the cell bodies of TG neurons.

Keywords CGRP, Migraine, Trigeminal ganglion, Alpha-CGRP, Beta-CGRP, Immunohistochemistry

Introduction

Migraine is a primary headache disorder that affects more than 10% of the global population [1, 2]. Though various studies have demonstrated that calcitonin gene-related peptide (CGRP) levels are elevated in migraineurs during migraine attacks and that targeting CGRP and its receptor with antibodies is effective in preventing and treating migraine in migraineurs [3–6], the molecular mechanism behind the role of CGRP in migraine is still to a large extent unknown. The high expression of CGRP and its receptor in the trigeminal ganglion (TG), along with evidence suggesting that migraine pain is mediated by TG neurons, has led researchers to propose that CGRP activity within the TG plays a significant role in migraine [7, 8].

CGRP is expressed as two isoforms, αCGRP and βCGRP, in several species, e.g. humans and rodents [9]. In addition to the expression in TG neurons, αCGRP and βCGRP are co-expressed in various cell types, especially in the nervous system. αCGRP shows higher expression levels in most sensory and motor neurons, while βCGRP is a key isoform expressed in neurons of the intestine [10, 11] although αCGRP can also be found, e.g., in intestinal immune cells [12]. In humans and mice both isoforms mature into peptides of 37 amino acids with high similarity, making it nearly impossible to produce antibodies that distinguish between the isoforms. For this reason, "CGRP" is often used to describe both isoforms [11, 13, 14]. Going further into the details of expression, mouse αCGRP and βCGRP are expressed from the *calca* and *calcb* genes respectively, both located on chr 7 in mice with both genes consisting of five similar exons. Due to the high similarity between *calca* and *calcb*, it is assumed that *calcb* has arisen from duplication and divergence of *calca* [15]. Calcitonin, a second peptide produced from *calca*, is not transcribed from *calcb* [16].

Focusing on the TG, both αCGRP and βCGRP are expressed as mRNA, with neurons expressing both isoforms being the most prevalent, and constitute 39% in mice and 37% in humans. Neurons expressing only αCGRP (28% in mice and 7% in humans), or only βCGRP (5% in mice, 16% in humans) are less common. Additionally, 28% of neurons in mice express neither peptide compared to a higher 39% in humans [17]. While the expression patterns of CGRP in the TG is well characterized, the mechanisms underlying their differential expression and processing within neurons remain unclear.

Both isoforms are expressed as pre-pro-peptides (pre-pro-αCGRP and pre-pro-βCGRP). Pre-pro-peptides contain an N-terminal hydrophobic signal peptide (pre-) that facilitates the transport of the nascent peptide to the ER. This signal peptide is cleaved off as translation terminates, resulting in the pro-peptide being translocated into the ER [18, 19]. From the ER the pro-peptides are transported through vesicular transport to the *cis* Golgi Apparatus. The pro-peptides move through the Golgi Apparatus where pH decreases, calcium increases and various peptidases are present [18, 20, 21]. Peptides destined for regulated secretion are packed into immature secretory granules from the *trans* Golgi network. The final sorting into secretory granules is thought to be regulated through protein aggregation and interactions with calcium ions [22, 23]. The immature secretory granules later mature into large dense core vesicles from which the mature peptide is secreted. The localization of the signal peptide, sorting peptide and mature peptide for αCGRP and βCGRP is visualized in Fig. 1A.

Along the secretory pathway the sorting peptide is cleaved off from the pro-peptide to produce a mature peptide (predicted enzymatic cleavage sites of pre-pro-αCGRP and pre-pro-βCGRP are shown in Fig. 1B). Enzymes important in this process are thought to be the two pro-peptide convertases (PCs) PC1 (also known as PC3 or PC1/3), PC2 and carboxypeptidase E (CPE) [24, 25]. PC1 and PC2 recognize mono- and dibasic cleavage sites (K/R or KK, KR, RK or RR) while CPE cleaves off C-terminal basic amino acid residues. A final important step involves peptidylglycine alpha-amidating monooxygenase (PAM) which replaces a C-terminal glycine with an amide, ensuring peptide stability.

In the current study, we set out to determine the protein expression of αCGRP and βCGRP to test the hypothesis that αCGRP and βCGRP localize differently within the neurons of the mouse TG. We apply immunohistochemistry (IHC) on αCGRP Knock Out (KO), Heterozygote (Het) and Wild Type (WT) animals, combined with a bioinformatical approach to deepen our understanding of CGRP in the trigeminovascular system.

Methods

Mice

Mice were maintained in a 12/12 h light-dark cycle with access to exercise equipment and food and water *ad libitum*. The mice were fed with SAFE A30 (Scientific Diet,

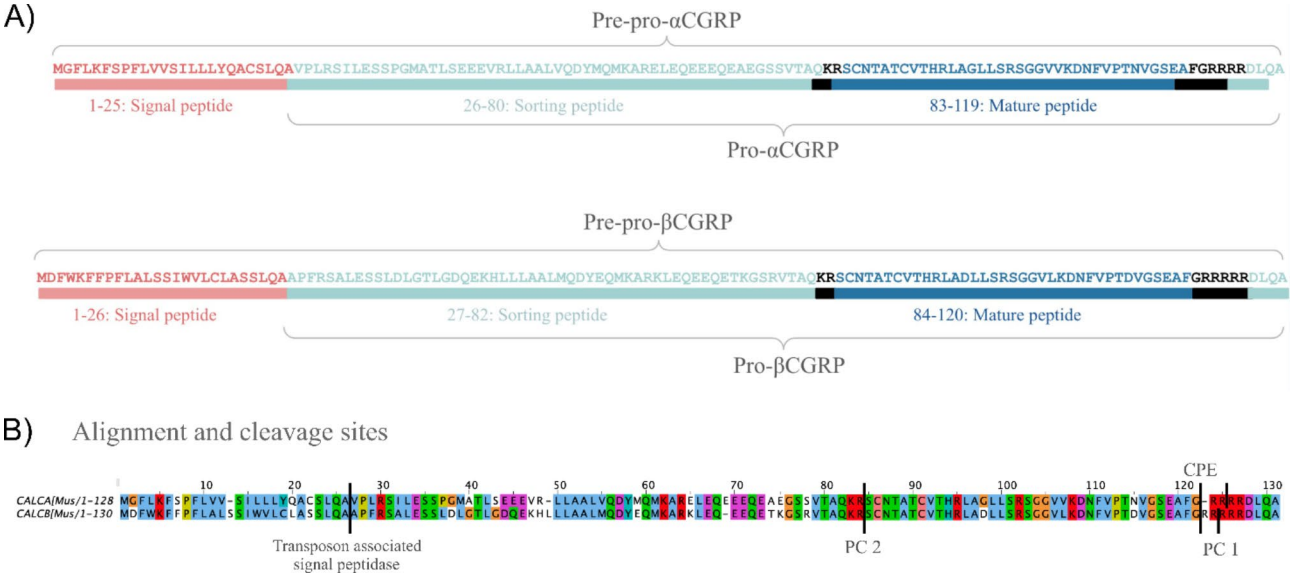

Fig. 1 Visual representations of pre-pro-αCGRP and -βCGRP primary structures. **(A)** Mouse pre-pro-αCGRP and pre-pro-βCGRP based of Uniprot predictions. **(B)** Visual representation of enzymatic cleave sites thought to be present in the mouse precursors. Cleavage sites of the translocon associated signal peptidases, prohormone convertase 1 (PC1), carboxypeptidase E (CPE) and prohormone convertase 2 (PC2) are indicated with black lines. The sequences are downloaded from NCBI (NP_001029126.1 and NP_473425.2), alignments are made in Jalview with Muscle with defaults, colored with Clustal (S10) and the possible cleavage sites are determined manually by comparison with amylin (NP_034621.1)

Germany). Only male mice were used in the current study, as mechanistic aspects of neuropeptide sorting, a process governed by conserved intracellular pathways are not expected to exhibit significant sex-specific differences. All experiments were approved by the Danish Animal inspectorate, license number 2023-25-0201-01469 and 2024-15-00202-00213.

WT mice ($n = 5$) were B6 mice purchased from Taconic, Ejby, Denmark. B6.Cg-Calca$^{tm1.1(cre/EGFP)Rpa}$/J mice produced by Carter and colleagues were purchased from the Jackson Laboratory [26], and are referred to as KO mice ($n = 15$). Het mice ($n = 5$) were made by breeding WT and KO mice and using the F1 offspring hereof (Fig. 2A). The KO mice are homozygous for an altered version of the *calca* gene where αCGRP-expressing cells express a myc-tagged, nuclear localization-tagged (NLS tagged) form of Cre: EGFP instead of αCGRP (Fig. 2B). The construct is inserted directly following the first start codon in the αCGRP gene, which is placed in the second exon and initiates translation of the pre-pro-peptide. This strain is a αCGRP KO, as the construct contains a polyadenylation site which causes transcription to terminate prior to the neuropeptide coding sequence.

TG dissection, fixation and sample preparation

15 fresh male mice (5 of each genotype), 5 KO male mice given a subcutaneous injection of 200 µl of 4,65 µg/µl, equating to 30 mg/kg, a well-established dosing regimen [27–30], of a monoclonal CGRP antibody (given 1 week before the mice where culled, fremanezumab [diluted in saline], Teva, Germany) and 5 KO male mice given a saline injection (treated for 1 week, sodium chloride, Fresenius Kabi, 9 mg/ml, Denmark), were sedated with gas (70% CO2 in 30% O2) followed by decapitation. The heads were placed in synthetic interstitial fluid (108 mM NaCl, 3.48 mM KCl, 3.5 mM $MgSO_4$, 26 mM $NaHCO_3$, 11.7 mM NaH_2PO_4, 1.5 mM $CaCl_2$, 9.6 mM Na^+ Gluconate, 5.55 mM Glucose, 7.6 mM Sucrose) after having skin and jaw removed. The skull was cut open and the brain removed to give access to the TGs. Both TGs (fresh animals) or the right TG (injection study) were dissected out and placed in paraformaldehyde (PFA) 4% in phosphate buffer 0.01 M pH = 7.2. After ~2 h, TGs were transferred to a Sörensen's phosphate buffer (0.028 M NaH_2PO_4, 0.072 M Na_2HPO_4) containing 10% sucrose and left overnight, before being transferred to a Sörensen's phosphate buffer containing 25% sucrose (up to 7 days). Gelatin medium (30% egg albumin and 3% gelatin in distilled water) was used for embedding. The TGs were kept at -80 °C until being sliced at 10 μm using a cryostat (Leica Biosystems, Germany). The sections were transferred to Superfrost Plus Microscope Slides (VWR, USA) and stored at -20 °C.

IHC

The area containing the sections where circled with a pap-pen (Vector laboratories, USA), and placed in a humidifying chamber. The sections were washed for 3 × 5 min with washing buffer containing 0.05% Tween20 in Phosphate Buffered Saline (PBS), followed by 20 min

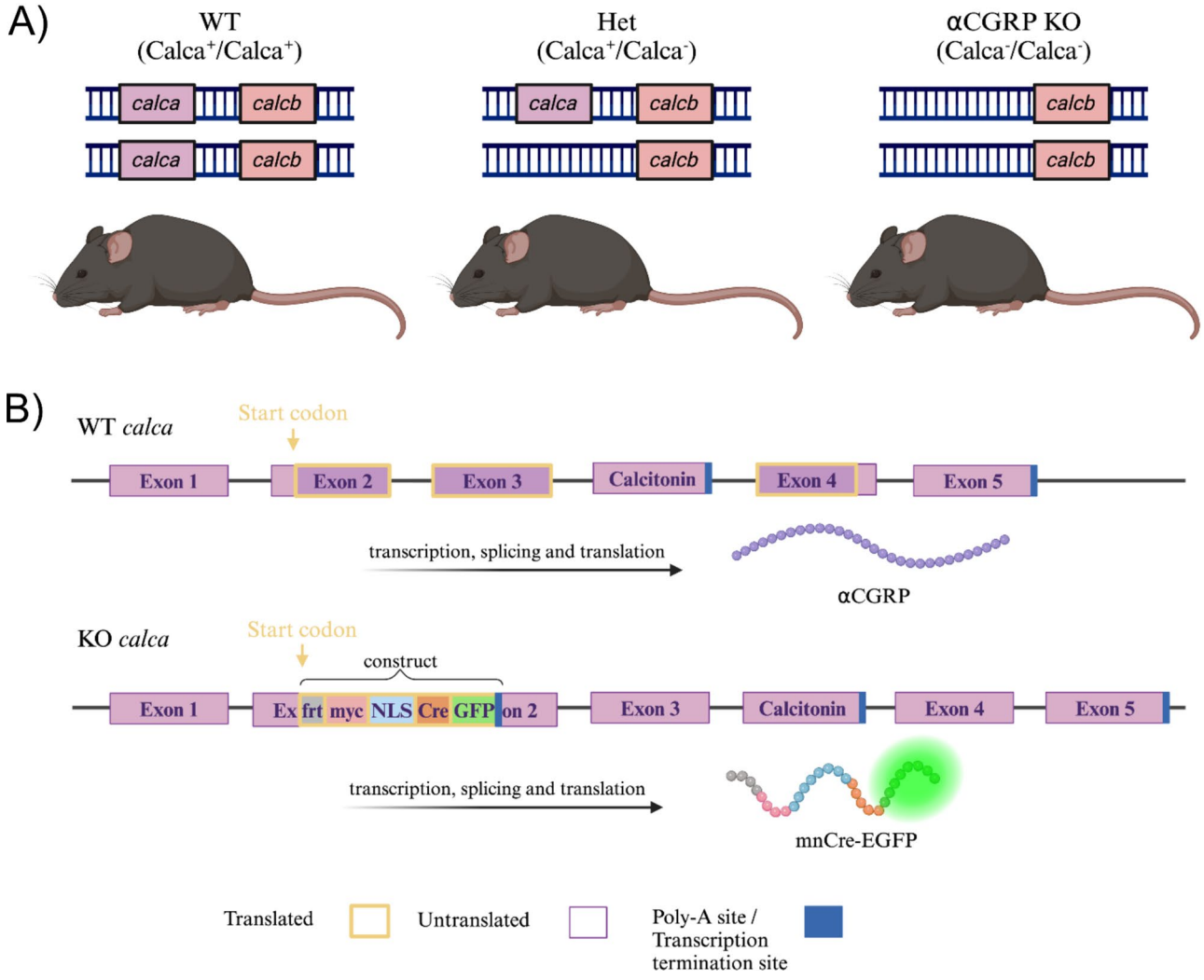

Fig. 2 Visual representations of applied mouse model and genetics. **(A)** Visual representation of the mouse model used in this article. The figure shows number of functional αCGRP coding genes (*calca*) and βCGRP coding genes (*calcb*) present in the three genotypes; wild type (WT), heterozygous (Het) and α CGRP KO. **(B)** Visual representation of the WT *calca* gene, the KO *calca* gene and the resulting peptides. The representations show the sequence spanning from nucleotide 114,225,223–114,236,145 on chromosome 7 in the mouse genome. mnCre-EGFP is short for myc-NLS-Cre-EGFP. Created in BioRender. Waever, S. (2025) https://BioRender.com/f20a252

in blocking buffer (0.3% Triton X-100, 3% BSA and 0.3 M glycine in PBS) and washed for 5 min with antibody diluent buffer (0.1% Triton X-100 and 1% BSA in PBS).

For the *mono-staining* for CGRP, TG sections were incubated with a primary antibody for CGRP (1:200, rabbit anti-CGRP (D5R8F), Cell Signaling USA) overnight at 4 °C. This antibody detects a human epitope surrounding Val_{32} in CGRP ($Val_{114,}$ in the pre-pro-CGRP) and was chosen, as it is a recombinant antibody, validated for IHC. In addition to this sequence being highly conserved between human and mouse pre-pro- α CGRP and - β CGRP (S1), the fact that it is recombinant means low lot-to-lot variation, allowing others to purchase the same antibody and reliably reproduce the results. The following day, the slides were washed 3 × 5 min with antibody diluent buffer. Slides were incubated for 1 h at room temperature with the secondary antibody (1:500, Goat anti-rabbit IgG Alexa 568, ab275471).

For the *double staining* with CGRP and pro-CGRP IHC, an antibody targeting an epitope located within the sorting peptide of human pro-calcitonin was used (1:2500, mouse-Anti-PCT mAB 42 cc, Cat. # 4PC47, Hytest Ltd, Turku, Finland). The sorting peptide of αCGRP and calcitonin are identical. There is larger variation in the sorting peptide, but the antibody was chosen as there is a large species similarity in the epitope region. The epitope within the sorting peptide of human pro-αCGRP share 15/19 amino acids with mouse αCGRP and 14/19 amino acids with mouse βCGRP (S1). The secondary antibodies

used for this IHC were Goat anti-Mouse IgG Alexa 568 (ab175473) and Goat anti-rabbit Alexa 488 (ab150077).

Following secondary antibody incubation, both above procedures were followed by a 3 × 5 min incubation with washing buffer and 1 min with deionized water to avoid formation of PBS crystals. Lastly, 1–2 drops of antifade mounting medium with DAPI (H-1200, Vectrashield) was added to each slide. The IHC results were viewed and photographed on a Nikon Eclipse Ti2 microscope.

Quantification and statistics

CGRP localization patterns were divided into 5 categories: CGRP-positive cells with small dots equally distributed, CGRP-positive cells with large dots equally distributed, CGRP-positive cells with dots in a circular formation, CGRP-positive cells that are all red and CGRP-positive cells with polarized CGRP distribution. Examples of the different localization patterns are shown in S2. For localization patterns, pictures were taken at intensities that resulted in the lowest number of overexposed cells while having the highest amount of CGRP-positive cells. We further counted: neuronal cell bodies, cells with green nuclei and CGRP-positive cells. The number of cell types were counted manually for every picture and the investigator was blinded for the injection study. The CGRP localization pattern counts were normalized by number of CGRP-positive cells in each frame. ImageJ was used to measure the intensity of IHC results. Count data and intensity results were analyzed in GraphPad Prism 10.1.2 and shown as average and standard error of the mean (SEM). For statistics we used one-way analysis of variance (ANOVA) or Student's T-test. One-way ANOVA was used when analyzing results from three groups and Student's T-test was used when analyzing results from two groups. A p-value < 0.05 was considered significant.

Bioinformatic analyses and predictions

Sequences of mouse (*Mus musculus*), human (*Homo sapiens*), rat (*Rattus norvegicus*), rhesus monkey (*Macaca mulatta*), zebrafish (*Danio rerio*), horse (*Equus caballus*) *and* wild boar (*Sus scrofa*) either or both α CGRP and β CGRP precursors were acquired from the NCBI protein database (NCBI Reference Sequence of pre--ro-*α*CGRP and pre-pro-*β*CGRP: NP_001029126.1 and NP_473425.2). Different alignments were produced in Jalview by MUSCLE with defaults. The alignments were colored to show identity, hydrophobicity, charged amino acids and with Clustal to show similarity.

The Peptide Calculator (Bachem) was used to predict isoelectric points of various maturation stages of *α*CGRP and *β*CGRP. The calculator predicts the pH at which the net charge of the given peptide is zero and states that the values are calculated by approximation with an accuracy of ± 0.01. Neurosnap was used to determine three-dimensional structures of various peptide sequences as the tertiary structures of *α*CGRP and *β*CGRP have not been determined experimentally at any maturation step. Neurosnap uses AlphaFold2 which is an artificial intelligence engineered to predict protein structures. Jumper et al. have demonstrated the accuracy of AlphaFold2 by comparing the artificial intelligently generated spatial structures of various proteins with their experientially determined structures [31].

Results

CGRP mainly localize in TG axons of αCGRP-expressing mice

We first set out to investigate whether *α*CGRP and *β*CGRP localize differently in neurons of mouse TGs using IHC on three different genotypes (WT, Het and KO). CGRP was found in cell bodies across WT (calca$^+$/calca$^+$), Het (calca$^+$/calca$^-$) and KO (calca$^-$/calca$^-$) mice ($n = 5$, Fig. 3), however, the overall intensity of the IHC was clearly different between the genotypes (see quantification later) (Fig. 3). While all genotypes are expected to express *β*CGRP, interestingly, we only detected clear CGRP presence in axons of *α*CGRP-expressing genotypes (WT and Het), indicating that *α*CGRP but not *β*CGRP localizes in the axons of TG neurons. Although we observed single CGRP-positive fibers in some KO TGs (S3), only in TGs from WT and Het mice, was CGRP consistently visible as beads on a thread continuously along nerve fibers. It is worth noting that in the Het TG axons the patterns were similar, but the intensity lower. All IHC data from this experiment can be found in S4 and S5. The finding that CGRP (assumed to be βCGRP) does not localize to the axons of KO mouse TGs indicates that *β*CGRP might not function as a typical neurotransmitter.

CGRP localize differently in neuronal cell bodies of KO and WT mice

As stated above, the overall expression of CGRP was evidently lower in the Het and KO TGs compared to WT TGs (S6). Pictures of WT TGs had an average intensity (Arbitrary Units, A.U.) of 12.8 ± 0.6, Het had an average intensity of 8.1 ± 0.4 and KO TGs had an average intensity of 5.2 ± 0.2, with intensities significantly different between all three genotypes ($p\text{-value}_{WT:\ Het} = 0.0007$, $p\text{-value}_{WT:\ KO} < 0.0001$, $p\text{-value}_{Het:\ KO} = 0.0068$) (Fig. 4A). Enhancing the exposure to study the detailed localization patterns of CGRP in the different genotypes, we chose to focus on a neuronal-body rich part of the TG. The number of neuronal nuclei was near identical in pictures acquired of WT (146.8 ± 19.9), Het (145.0 ± 12.8) and KO (143.8 ± 16.0) TGs.

The number of cells containing small equally distributed CGRP formations within these pictures was similar

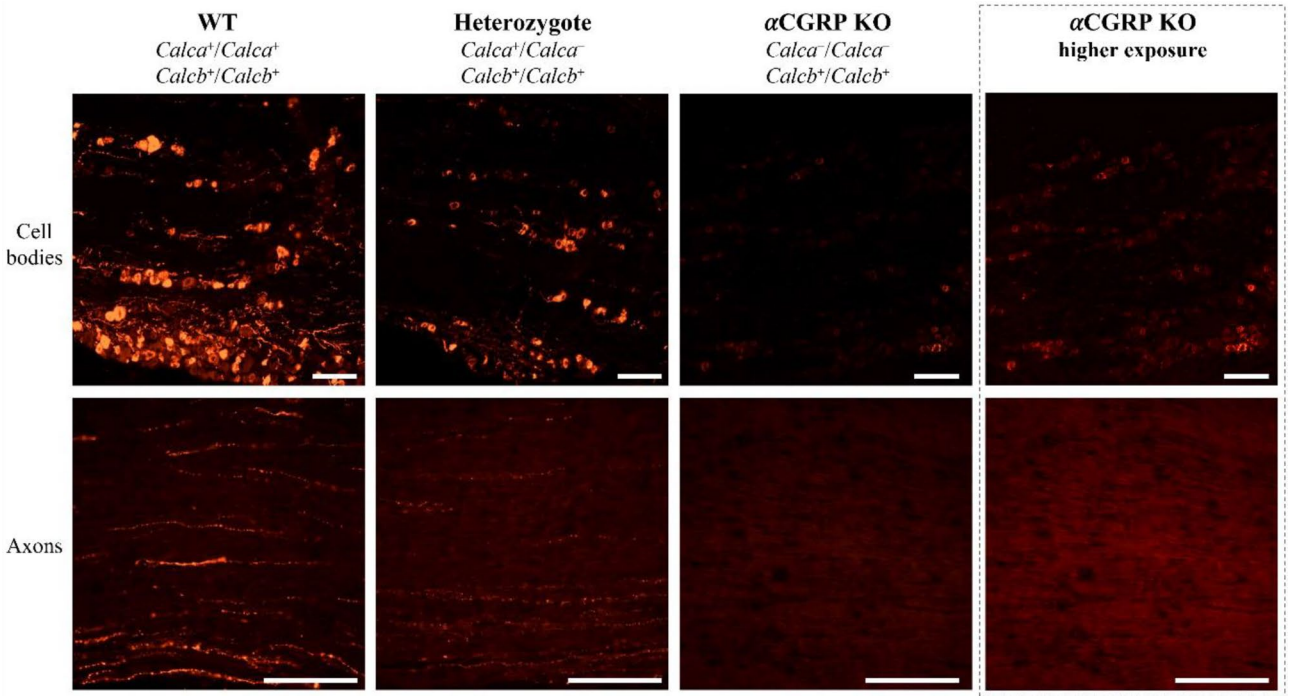

Fig. 3 CGRP localization in mouse TG neurons. Immunostaining of TGs from WT, Het and KO mice targeting CGRP. Pictures were taken at 40 ms in areas with large concentration of cell bodies and at 200 ms in areas with a large concentration of axons. The pictures have hence been adjusted equally to intensify signals (higher exposure pictures (outlined by dashed line) are adjusted differently from the other pictures). CGRP is visualized in red by immunostaining with a primary antibody targeting CGRP (D5R8F) and a secondary antibody conjugated to Alexa568. Scalebars are 100 µm

between WT (34.1 ± 9.0) and Het (36.9 ± 6.6) but significantly different between WT and KO (56.1 ± 11.0, $p = 0.025$) (Fig. 4B). The number of all red cells was significantly different between WTs (15.8 ± 3.1) and KOs (6.7 ± 1.4) ($p = 0.040$) but not different between Het (10.0 ± 1.9) and the other genotypes ($p_{WT:\ Het}=0.214$, $p_{Het:\ KO}=0.578$) (Fig. 4C). The number of cells showing large formations of CGRP was not significantly different ($p = 0.386$) between WT (37.2 ± 4.4) and KO (25.4 ± 5.4), but showed larger variation. No significant difference was obtained when comparing number of cells showing the other localization patterns in different genotypes (small dots: $p_{WT:\ Het}=0.925$, $p_{Het:\ KO}=0.059$, circular formation: $p_{WT:\ Het}=0.127$, $p_{WT:\ KO}=0.896$, $p_{Het:\ KO}=0.255$, large dots: $p_{WT:\ Het}=0.897$, $p_{Het:\ KO}=0.555$, polarized localization: $p_{WT:\ Het}=0.749$, $p_{WT:\ KO}=0.600$, $p_{Het:\ KO}=0.966$) (Fig. 4D-F).

Furthermore, the relative distribution of each localization pattern within each genotype was analyzed (Fig. 5A). KO TGs contained the highest percentage of cells with small CGRP localizations (56%), Het the second most (37%) and WT the least (34%). The highest percentage of the large localization pattern was observed in WT TGs (37%) and the fewest in KO TGs (25%). Therefore, β CGRP, (the only isoform in KO TGs), mainly locate in smaller patterns while α CGRP (predominant isoform in WT TGs) tends to localize in larger formations or cause the cell bodies to appear all red.

TG neurons isolated from Het mice, expressing both αCGRP and mnCre-EGFP (neurons with green nuclei where αCGRP is currently expressed) were counted to investigate cells known to specifically express αCGRP (Fig. 5B). In these cells CGRP was mainly observed to locate in large formations (44%). There was a significant difference between the number of cells containing CGRP in large formations (10.2 ± 2.4) compared to circular formations (2.2 ± 0.7, $p = 0.005$), compared to all red cells (3.2 ± 1.2, $p = 0.014$) and compared to polarized CGRP localization (2.2 ± 0.7, $p = 0.005$), but not compared to small formations (5.6 ± 2.5, $p = 0.169$). Combined, these data support that αCGRP both localizes in large formations within neuronal cell bodies, and contributes to the all red cells.

KO mice subcutaneously injected with CGRP antibody still contain CGRP-positive TG neurons

KO mice were injected with 30 mg/kg CGRP monoclonal antibodies (fremanezumab), which would bind plasma βCGRP, thus eliminating potential enteric βCGRP uptake in the TG. For these mice the IHC appeared similar between the antibody and saline treated animals (S8). No striking difference in either intensity or localization patterns were observed. For the percentage of CGRP-positive cells per neuronal cell bodies, no significant difference ($p = 0.48$) was found between the treated group

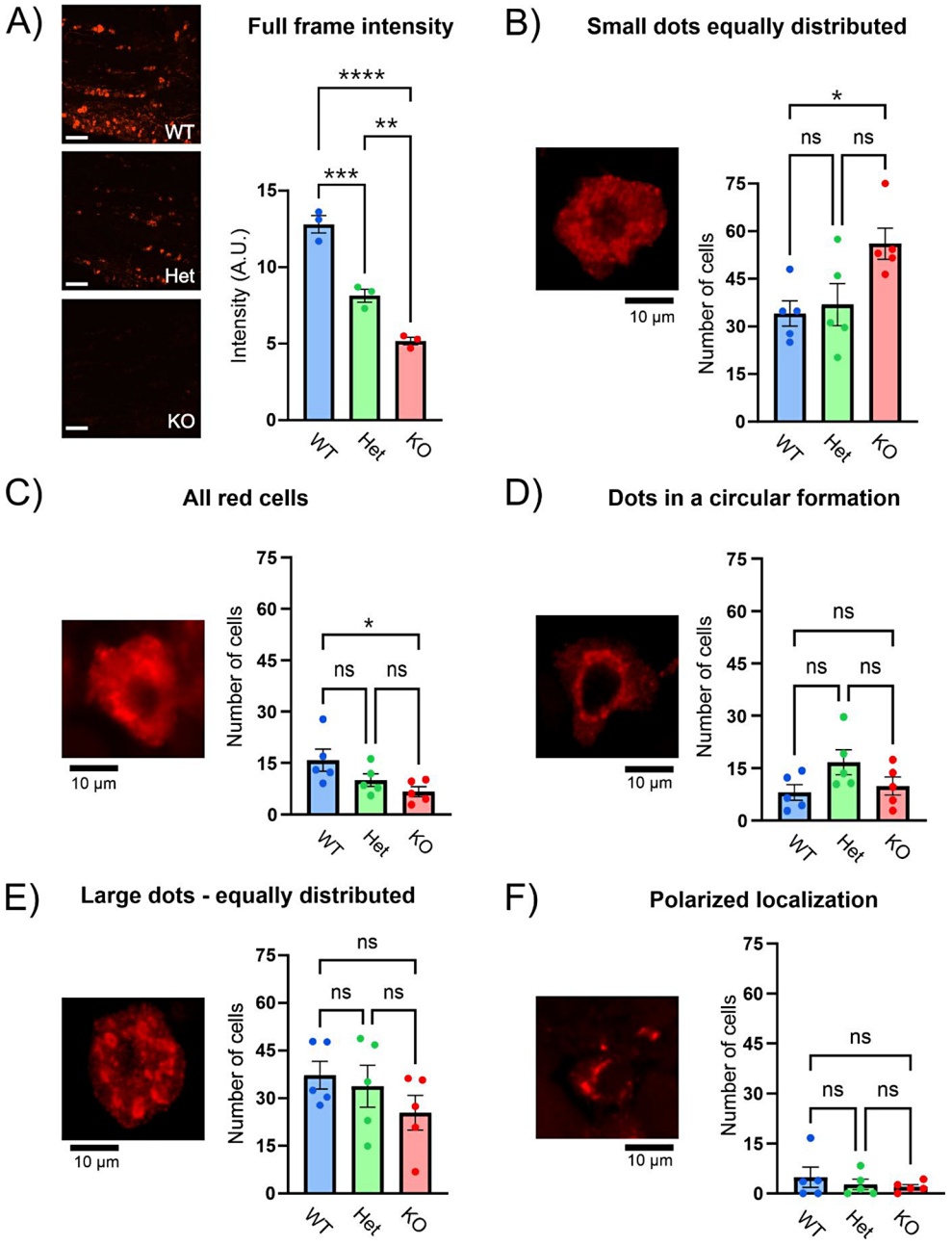

Fig. 4 CGRP IHC intensity measurements and quantification of CGRP localization patterns. **A)** Average intensities of TG CGRP signals (D5R8F, red, alexa568) from the full frame of WT TG ($n=3$), Het ($n=3$) and KO ($n=3$). Intensity is measured in grayscale arbitrary units, and a representative picture of each genotype is shown. **B-F)** Graphs showing average number of different localization patterns (S7) observed in pictures of WT, Het and KO TGs (each $n=5$). An example of the localization pattern can be found next to the graph. * p-value $\leq$ 0.05, ** p-value $\leq$ 0.01, *** p-value $\leq$ 0.001 and **** p-value $\leq$ 0.0001. Scalebars are 100 µm in A, or 10 µm as indicated

(44.8 ± 6.6%) and the control group (39.0 ± 4.1%, Fig. 6A), indicating that βCGRP, is synthesized within the TG neurons. Figure 6B shows a representative picture of a TG from a control and a fremanezumab treated mouse.

Both the CGRP observed in WT and KO TG neuronal cell bodies contain the CGRP sorting peptide

The above experiment showed that βCGRP observed in TG neurons is mainly or solely produced by the neurons themselves. To confirm this synthesis, IHC experiments with antibodies recognizing mature CGRP and the sorting peptide of pro-CGRP were conducted. Figure 7 shows examples of the resulting co-staining in a WT and KO

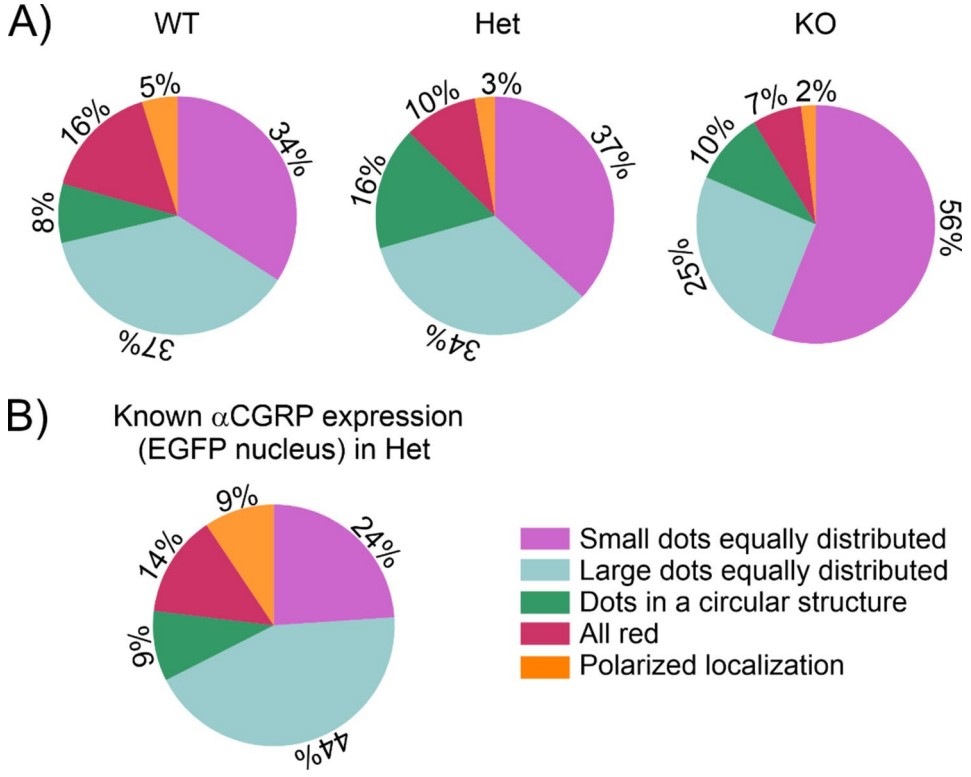

Fig. 5 CGRP localization pattern distributions in TGs of WT, Het and KO mice. **(A)** Pie charts showing the average percentage of different CGRP localization patterns in immunostainings of WT, Het KO TGs (each $n = 5$). **(B)** Pie chart showing the average percentage of different CGRP localization patterns in cells with EGFP in nucleus from immunostainings of five TGs from Het mice

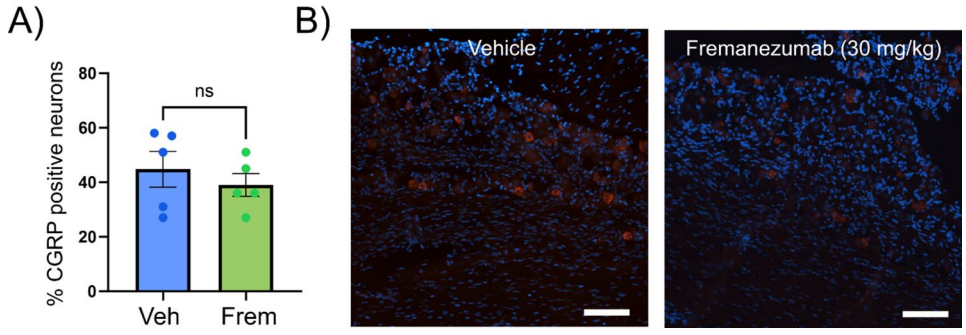

Fig. 6 CGRP-positive cells in mice injected with Fremanezumab or saline. **(A)** Graph showing percentage of CGRP-positive cells (D5R8F, red, alexa568) pr neuronal cell bodies in control mice (injected with saline (Veh)) compared to treated mice (injected with CGRP antibody (Frem)). No significant difference (ns) was observed between the two groups. **(B)** Examples of two immunostainings with CGRP antibody (D5R8F) and DAPI used for quantification. CGRP is shown in red and cell nuclei in blue. Scalebars are 100 µm

mouse. All IHC results can be found in S9. Formations of a clear sorting peptide pattern can be observed within cell bodies which match the formations of CGRP. These patterns are observed in both WT and KO mice suggesting, that the two epitopes are present on the same peptide or peptides near each other in both genotypes. These results thus indicate that the sorting peptide is found together with the neuropeptide sequence within the neuronal cell bodies of KO mice and conclude that all or most βCGRP observed within TG neurons is produced by the neurons themselves.

Mouse pre-pro-α- and pre-pro-βCGRP fold into similar secondary and tertiary structures

The factors influencing protein localization are often embedded within the primary, secondary, or tertiary structure of the peptide. Since neither αCGRP nor βCGRP forms quaternary structures, the tertiary and secondary structures of both peptides were analyzed to

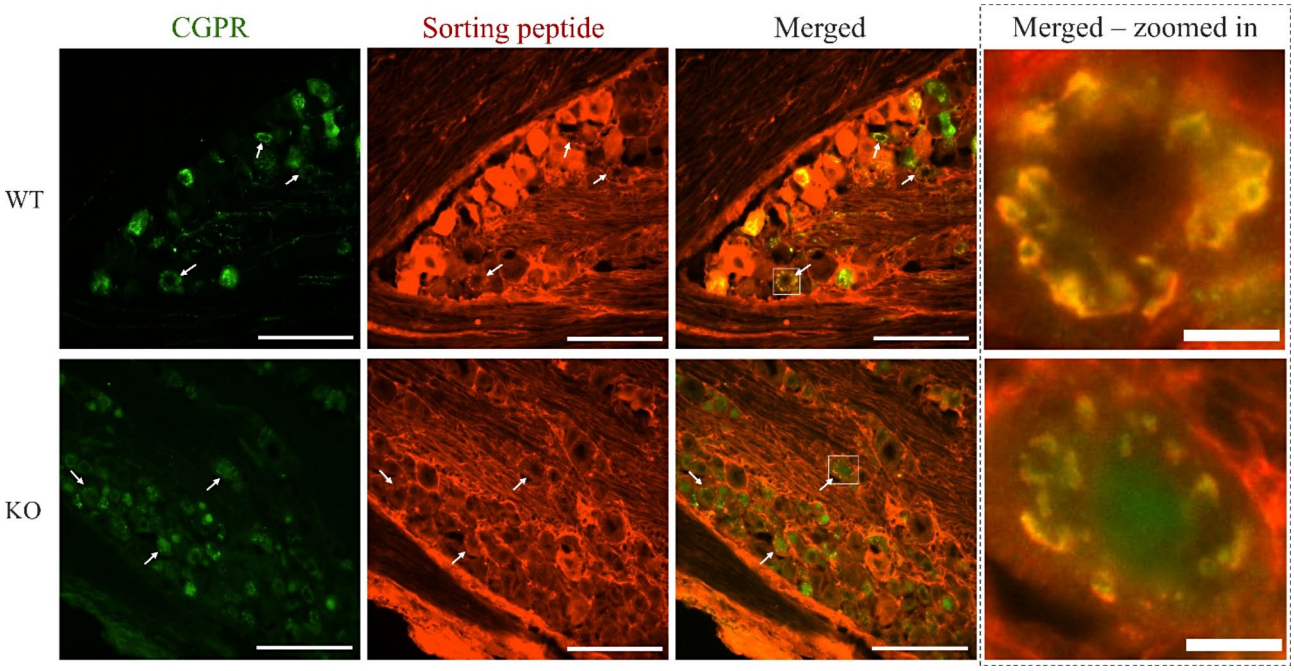

Fig. 7 CGRP and CGRP sorting peptide localization within WT and KO mouse TG neurons. Examples of IHC of either WT or KO mouse TGs with an antibody recognizing the neuropeptide sequence of CGRP (D5R8F green, alexa488) and the sorting peptide sequence (42 cc, red, alexa568). White arrows point to signals that are seen in both colors. Overlapping signals appear yellow in the merged figures. The rightmost panel shows a sample cell (from the white squares). Scalebars are 50 µm–10 µm in the inserts

determine whether their folding could provide insights into the observed differences.

The site Neurosnap predicted that both pre-pro--CGRP and pre-pro-*β*CGRP contain three alpha helices connected by unstructured elements (Fig. 8A). The first alpha helix, which is located at the N-terminal contains the signal peptide and is placed in an almost 90-degree angle compared to the rest of the peptide in both isoforms. When entering the sequences of pro-*α*CGRP and pro-*β*CGRP into Neurosnap, two similar structures were generated (Fig. 8B). Both structures contain two alpha helices, connected and flanked by disordered stretches. All hypothesized cleavage sites were predicted to localize within unstructured parts of the peptide (Fig. 8B). Tertiary structural differences between the two peptides do not seem to explain the differentiating localization patterns.

Mouse pro-α- and pro-βCGRP contain different sorting peptides

As the analysis of αCGRP and βCGRP secondary and tertiary structure did not indicate significant differences, we examined the primary structures, to investigate potential differences. The hydrophobicity of pre-pro-*α*CGRP and pre-pro-*β*CGRP is highly similar from amino acid 83/84–128/130 (corresponding to the mature neuropeptide and C-terminal pro-peptide sequence) but differs more in the other parts of the sequence, as shown in the alignment of the amino acid sequences (Fig. 9A). Pre--ro contains more charged amino acid residues ($n_{\text{positively charged residues}}$=18 and $n_{\text{negatively charged residues}}$=16) compared to pre-pro-*α*CGRP ($n_{\text{positively charged residues}}$=14 and $n_{\text{negatively charged residues}}$=15).

The pre-pro-peptides are highly similar from amino acid residue 83/84 to the C-terminal as shown by Clustal X Color Scheme (only three dis-similarities). The rest of the sequences have lower identity especially from amino acid 10–50, but some similarity in amino acid profiles. Interestingly, the sequences corresponding to the sorting peptides (26/27–80/82) are notably different. To investigate whether the mismatches in the sorting peptides are due to evolutionary insignificance of the sequences and therefore high mutation rate, or evolutionary significance for the biological function, alignments were made between pre-pro-αCGRP and -βCGRP sequences in 5 different species (Fig. 9B and C). The sorting peptides of αCGRP show high similarity while the sorting peptide of βCGRP varies more between species. In the alignment of pre-pro-αCGRP homologs, 21 instances of non-conserved amino acids and gap openings were identified (38%) where 29 (52%) were counted for pre-pro-βCGRP homologs. If only counting non-conservative amino acids (and gap openings), when the conservation is lacking in more than one species, only 9 instances are observed in pre-pro-αCGRP homologs (16%) where 20 are found in pre-pro-βCGRP homologs (36%).

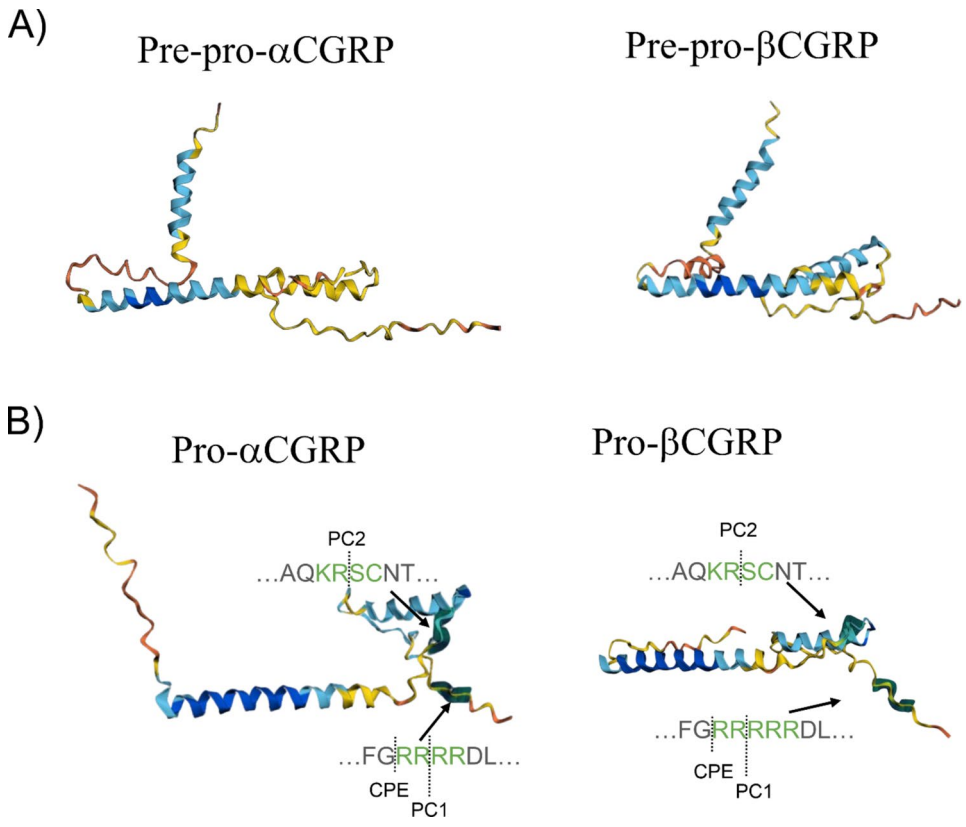

Fig. 8 Predicted tertiary structures of pre-pro-αCGRP and pre-pro-βCGRP. **A**) Tertiary structures of mouse pre-pro-α CGRP and pre-pro-β CGRP produced by AlphaFold2 from the web page NeuroSnap. Colors indicate model confidence. **B)** Tertiary structures of mouse pro-α CGRP and pro-β CGRP produced by AlphaFold2 from the web page NeuroSnap. Colors indicate model confidence. In green is highlighted PC2, CPE and PC1 cleavage sites

Furthermore, the long insertion in rat pre-pro-βCGRP is striking. These data show that the sorting peptide is more conserved in αCGRP (indicating biological importance) than in βCGRP (indicating less or no biological importance).

Differences in the sorting peptide give different isoelectric points

Since the key difference between αCGRP homologs and βCGRP homologs is the primary structure of the pro-peptide, we hypothesized that there could be a key difference in their isoelectric points, which has been shown to be a key in peptide sorting and aggregation [32]. The isoelectric points of the pro-peptides before and after cleavage and modification by PC1, PC2, CPE and PAM were predicted by the Peptide Calculator (Bachem). Pro-αCGRP is predicted to have a lower isoelectric point than pro-βCGRP after losing the signal peptide (isoelectric point$_{\text{pro-αCGRP}}$=5.42, isoelectric point$_{\text{pro-βCGRP}}$=8.95) meaning that αCGRP would be positively charged in the acidic environment of the *trans* Golgi network while βCGRP would be negatively charged. This difference in overall charge is predicted to continue until the sorting peptide is cleaved off by PC2 where the isoelectric point of pro-αCGRP increases by 4.32 while the isoelectric point of pro-βCGRP increases by 0.84.

After this cleavage, both isoforms will be negatively charged in the *trans* Golgi network. This shows that the differing sorting peptides greatly affect the charge of pro-αCGRP and pro-βCGRP and constitute a key difference between the two isoforms. For the mature peptide, αCGRP has a higher isoelectric point than βCGRP (isoelectric point$_{\text{-αCGRP}}$=9.15, isoelectric point$_{\text{-βCGRP}}$=7.00). Under the assumption that the order of enzymatic reactions is PC1, CPE, PAM and CP2, as seen with amylin [33], αCGRP will thus initially be negatively charged in the acidic environment of the secretory pathway, whereas βCGRP will continue to be positively charged (Table 1).

Discussion

In the current paper, CGRP was observed within cell bodies of all three genotypes of mice (WT, Het and KO) while CGRP localization within TG axons was only observed in αCGRP-expressing genotypes (WT and Het). These data indicate that both CGRP isoforms localize within neuronal cell bodies of the TG neurons, but only αCGRP localizes to the TG axons. In WT and Het TGs, we detected αCGRP in large parts of the cytosol, or in larger formations in the neuron. In the KOs, the cells

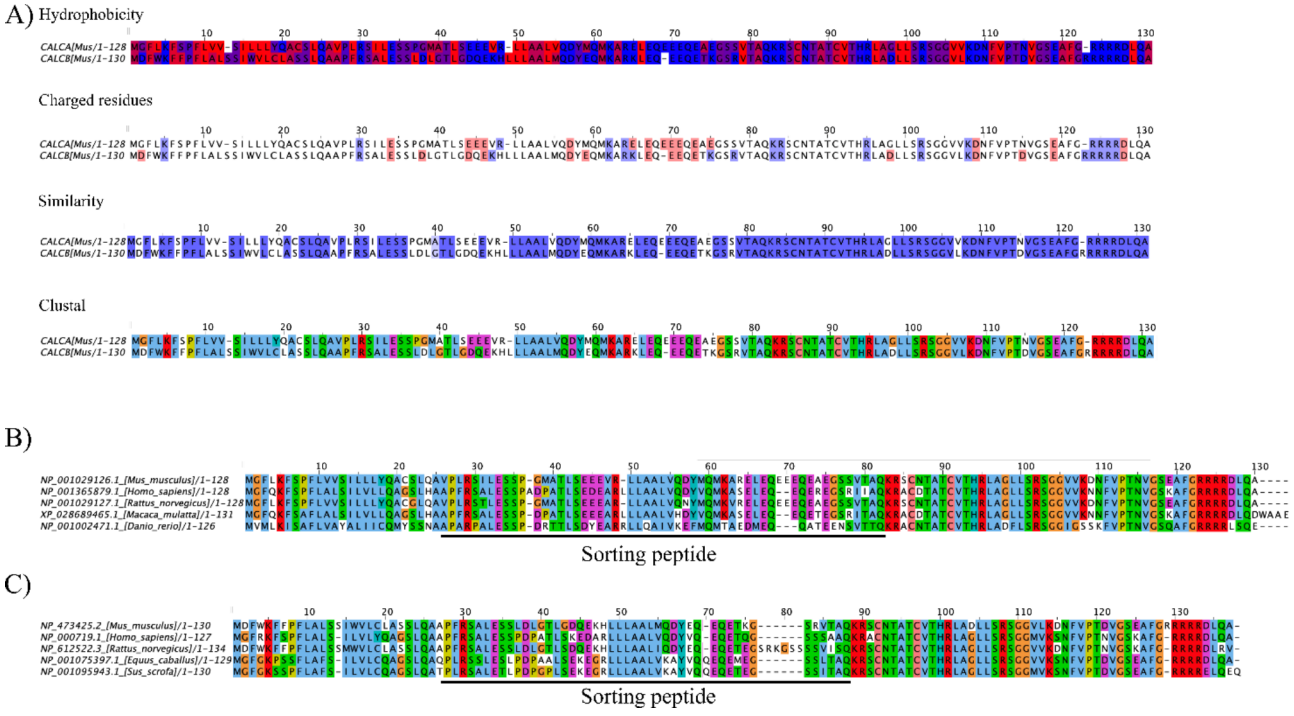

Fig. 9 Alignments of pre-pro-αCGRP and pre-pro-βCGRP in multiple species. **A)** Alignments of mouse pre-pro- α CGRP (*CALCA*) and pre-pro- β CGRP (*CALCB*) made with Jalview and colored to show similarity, hydrophobicity, charged residues and Clustal X default coloring. Dark blue indicates 100% similarity in the similarity coloring. Blue indicates hydrophobicity and red indicated hydrophilicity in the hydrophobicity coloring. Positively charged residues are colored blue and negatively charged residues are colored red in the charged residues coloring. A table describing Clustal X default coloring can be found in S10. **B)-C)** Alignments of (**B**) α CGRP and (**C**) β CGRP precursors in different species. Alignments were produced in Jalview with MUSCLE with default and colored with Clustal. Alignments for α CGRP was performed between mouse [Mus_musculus], human [Homo_sapiens], rat [Rattus_norvegicus], rhesus monkey [Macaca_mulatta] and zebrafish [Danio_rerio] α CGRP precursors. Alignments for β CGRP was performed between mouse [Mus_musculus], human [Homo_sapiens], rat [Rattus_norvegicus], horse [Equus_caballus] and pig [Sus_scrofa] β CGRP precursors. The sorting peptide sequences are indicated

Table 1 Isoelectric points of αCGRP and βCGRP at different maturation points. Isoelectric points of pro-α- and -βCGRP at different maturation steps. Red indicates a positive charge and blue a negative charge at pH∼6 equivalent to that of the *trans* golgi network

	αCGRP	βCGRP
Pro-	5.42	8.95
Post PC1	4.98	7.14
Post PC1, CPE and PAM	4.83	6.16
Post PC1, CPE, PAM and PC2	9.15	7.00

with CGRP in the entire cytosol were reduced, and the CGRP formation appeared smaller and more widespread in the cytosol. Co-localizing of mature CGRP and pro-CGRP in KO TG neurons, shows that βCGRP is not only transcribed in the TG neurons, but also translated into a peptide. This will be discussed in depth below.

One key finding is that αCGRP is the only isoform that localized to the axons of TG, demonstrating its transport along axonal pathways for potential neurotransmission (Fig. 3). In contrast, IHC performed on TGs from αCGRP KO mice, showed that βCGRP mainly appeared to reside in the neuronal cell bodies (although it is likely normally co-expressed with αCGRP) and not in the neuronal axons as the typical neurotransmitter (Fig. 3). Due to the specific cytosolic pattern, and that βCGRP is known as an enteric peptide, we hypothesized that βCGRP in the TG (through endosomal or receptor-mediated uptake), potentially could originate from enteric sources. Furthermore, CGRP (undetermined isoform) is detected in blood samples from patients [3, 10] illustrating that βCGRP could originate from the periphery. We therefore injected αCGRP KO mice with a monoclonal CGRP antibody, which should bind most of the circulating βCGRP. We observed no changes in the IHC between control and treated groups, supporting that βCGRP is produced in the TG (Fig. 6A-B and S8). This was further strengthened by the co-localization of CGRP and an antibody targeting the sorting peptide, which is produced during peptide

synthesis (Fig. 7). With the data presented in this study, we show for the first time, strong evidence for translation of the βCGRP peptide in the TG.

The distinct localization patterns of CGRP isoforms within the TG may indicate specialized roles for αCGRP and βCGRP in neuronal function. We speculate that the cells that contain βCGRP, might use CGRP (and particularly βCGRP) as a different type of secretory peptide, more like a hormone. αCGRP is the predominant isoform in TG, however, current antibody treatments target both isoforms, leaving it unclear whether βCGRP alone, or together with αCGRP, might play a causative role in migraine. Investigating these differences further could enhance understanding of their mechanistic contributions in migraine.

Looking into the details of the CGRP and pro-CGRP co-staining, the epitopes of the sorting peptide and CGRP are located near each other but do not show the exact same patterns (Fig. 7). We find three likely explanations hereof; firstly, the pro-peptide might be folded in a way that causes the epitope-binding antibodies to orient in opposite directions. Secondly, binding of one antibody might result in such steric hindering that a second antibody cannot bind to the same peptide. Thirdly, different parts of the pro-peptide might bind either enzymes or membranes during the maturation process and transport through the secretory pathway, resulting in the antibodies not being able to bind parts of the pro-peptides at given states. The interaction with enzymes, could be an interesting avenue of further research, particularly with focus on the Golgi structures.

In the Golgi, folding and sorting dynamics are affected by the peptide structure and we analyzed this in depth using a bioinformatical approach. In the performed 3D analysis, both pre-pro-αCGRP and -βCGRP were predicted to contain an alpha-helical signal peptide oriented in a roughly 90-degree angle compared to the rest of the peptide (Fig. 8A). This arrangement seems physiologically relevant, as the signal peptide is known to be integrated into the ER membrane during co-translational translocation and is cleaved off post-translation [18, 19]. The signal peptide likely orients away from the remainder of the peptide, facilitating its integration into the membrane and subsequent cleavage. The PC2 cleavage site was predicted to be located in between two other alpha helices in both pro-αCGRP and pro-βCGRP, which could regulate PC2 cleavage (Fig. 8B).

The lack of differences in the 3D structure led us to look into the primary structure (Fig. 9). Differences in the sorting peptides between the isoforms stood out, and particularly the estimated difference in the isoelectric points of αCGRP and βCGRP (Table 1). We therefore hypothesize that the differences between the sorting peptides and the effect on isoelectric points result in differential sorting of the two isoforms in the *trans* Golgi network. Sorting of peptides into secretory vesicles has been linked to protein aggregation, calcium binding, and interaction with sorting receptors, determining whether or not they are transported to the neuronal synapses [22, 34]. Through the *trans* Golgi, the pH decreases, and calcium levels increase, where the sorting peptides will cause the two peptides to behave differently [21, 23].

In most cells, the pH in the secretory pathway decreases from ~7.4 in the ER to ~6.0 in the *trans* Golgi network and ~5.5 in the secretory vesicles [21]. As seen in Table 1, αCGRP has a lower isoelectric point than βCGRP before PC2 cleavage, causing the peptides to have different overall charges. As the pH approaches the isoelectric point, the lack of net charge minimizes electrostatic repulsion between molecules, promoting aggregation or precipitation. This aggregation is believed to be important for packaging of neuropeptides [22, 34]. βCGRP, with its isoelectric point always staying above pH 7, will have a neutral net charge very early in the Golgi, potentially aggregating earlier than αCGRP. This is in our opinion the most likely explanation of why βCGRP never enters the large dense core granules and is not transported to the synapse.

Worth noting is the occasional single CGRP-positive fiber in some of the KOs (Fig. S3). Although this could be caused by differences in the pH in some single neurons, the most likely explanation is that our KO model is not a full/classical KO of the *calca* gene. The KO mice still contain the *calca* gene, but the inserted construct prevents αCGRP expression through the presence of a polyadenylation site just upstream of the translation initiation site. The Jackson Laboratory (ref. Strain #:033168), states that homozygote KO mice have "no (or greatly reduced) expression" of *calca*, indicating occasional αCGRP transcription could be present in KO mice [26]. This mechanism is similar to the transcription difference between calcitonin and CGRP, where a polyadenylation site is skipped and transcription continued [5, 35].

Limitations in the current study include the use of only male mice. However, the focus of the study is on the mechanistic aspects of neuropeptide sorting, a process governed by conserved intracellular pathways that are not expected to exhibit significant sex-specific differences. Thus, the use of male mice is unlikely to affect the validity of the findings or their generalizability to both sexes. Future studies investigating female mice would be valuable, particularly to explore potential implications of sex-specific differences in CGRP-related functions.

Further, for the 3D modelling, the major limitation with AlphaFold2 is that the predicted structures are based on crystal structures and thus represent the construction of the peptides under crystalized conditions. The predictions do thus not take into account the pH and

concentration of various minerals such as calcium which vary greatly throughout the secretory pathway and could alter the peptide structure. Pre-pro-αCGRP and -βCGRP show high tertiary and secondary similarity at the conditions set by AlphaFold2. However, Alphafold predicts the structure at neutral pH. It is unknown how the structures might change their alpha helices at lower pH due to their differences in isoelectric points. Park et al. have demonstrated how pH greatly changes the percentage of alpha helices in the common secretory vesicle cargo protein secretogranin II through circular dichroism [36]. The percentage of alpha helical structures was also shown to be larger when mimicking the trans Golgi network (pH 5.5) compared to mimicking the cytosol (pH 7.5), with the presence of alpha helices increasing the likelihood of peptides being sorted into secretory [37].

Translation challenges apply when comparing the human and mouse CGRP pre-pro-peptides, as they have some clear differences. Both human βCGRP and human αCGRP exhibit an isoelectric point above neutral, unlike their mouse counterparts. This difference is largely attributed to variations in the sorting peptides between the two species. We postulate that these differences are mitigated by phosphorylation, the most common mechanism for altering the charge of amino acids. There are several kinases present in the Golgi apparatus [38, 39], and these modifications may result in similar charge profiles. The possibility of phosphorylation in the Golgi of CGRP warrants further investigation.

Conclusion

In this study it was found that αCGRP is the main CGRP isoform to localize within the axons of mouse TG neurons, while βCGRP mainly localize within the neuronal cell bodies. Furthermore, βCGRP showed separate localization patterns compared to αCGRP, and was confirmed to be actively produced in TG neurons. Bioinformatical analyses showed that αCGRP and βCGRP contain differences in their sorting peptides (affecting the isoelectric point), but share common secretory enzymatic cleavage sites and tertiary structure.

Abbreviations

CGRP	calcitonin gene related peptide
CPE	carboxypeptidase E
Het	heterozygote
IHC	immunohistochemistry
KO	knock out
PAM	peptidylglycine alpha-amidating monooxygenase
PC1	pro-peptide convertase 1
PC2	pro-peptide convertase 2
TG	trigeminal ganglion
WT	wild type

Supplementary Information

The online version contains supplementary material available at https://doi.org/10.1186/s10194-024-01945-6.

Supplementary Material 1

Acknowledgements

We thank Philip V. Reducha for assistance in the blinding procedure, and Sara Stefansen for assistance with the animals.

Author contributions

S. L. Wæver: Conceptualization, Data curation, formal analysis, investigation, methodology, visualization, writing – original draft, writing – review and editing. K. A. Haanes: Conceptualization, data curation, formal analysis, funding acquisition, investigation, methodology, project administration, resources, supervision, visualization, writing – substantial review and editing. Both authors reviewed and edited the manuscript.

Funding

KAH was supported by a Lundbeck foundation Fellowship (R345-2020-1977). The funders had no role in study design, data collection and analysis, decision to publish, or preparation of the manuscript.

Data availability

Data is provided within the manuscript or supplementary information files.

Declarations

Ethics approval and consent to participate

The animal part of the study followed the guidelines of the European Communities Council (86/609/ECC) and was approved by the Danish Animal inspectorate, license number 2023-25-0201-01469 and 2024-15-00202-00213. All animal experiments were therefore performed in accordance with the European Community Council Directive on 'The Protection of Animals Used for Scientific Purposes' (2010/63/EU).

Consent for publication

Not applicable.

Competing interests

The authors declare no competing interests.

Author details

[1]Sensory Biology Unit, Translational Research Center, Rigshospitalet, Glostrup, Denmark
[2]Department of Biology, University of Copenhagen, Copenhagen, Denmark
[3]Danish Headache Center, Department of Neurology, Copenhagen University Hospital – Rigshospitalet, Glostrup, Denmark

Received: 5 December 2024 / Accepted: 30 December 2024
Published online: 14 January 2025

References

1. Bigal ME, Lipton RB (2009) The epidemiology, burden, and comorbidities of migraine. Neurol Clin 27:321–334
2. 2 Edvinsson L, Haanes KA (2021) Identifying New Antimigraine targets: lessons from Molecular Biology. Trends Pharmacol Sci 42:217–225
3. Goadsby PJ, Edvinsson L, Ekman R (1990) Vasoactive peptide release in the extracerebral circulation of humans during migraine headache. Ann Neurol 28:183–187
4. Olesen J, Diener HC, Husstedt IW, Goadsby PJ, Hall D, Meier U, Pollentier S, Lesko LM, Group BBCPoCS (2004) Calcitonin gene-related peptide receptor antagonist BIBN 4096 BS for the acute treatment of migraine. N Engl J Med 350:1104–1110
5. Rosenfeld MG, Mermod JJ, Amara SG, Swanson LW, Sawchenko PE, Rivier J, Vale WW, Evans RM (1983) Production of a novel neuropeptide encoded by the calcitonin gene via tissue-specific RNA processing. Nature 304:129–135
6. Silberstein SD, Dodick DW, Bigal ME, Yeung PP, Goadsby PJ, Blankenbiller T, Grozinski-Wolff M, Yang R, Ma Y, Aycardi E (2017) Fremanezumab for the Preventive treatment of chronic migraine. N Engl J Med 377:2113–2122

7. Haanes KA, Edvinsson L (2019) Pathophysiological mechanisms in Migraine and the identification of new therapeutic targets. CNS Drugs 33:525–537
8. Edvinsson L, Haanes KA, Warfvinge K, Krause DN (2018) CGRP as the target of new migraine therapies - successful translation from bench to clinic. Nat Rev Neurol 14:338–350
9. Russell FA, King R, Smillie SJ, Kodji X, Brain SD (2014) Calcitonin gene-related peptide: physiology and pathophysiology. Physiol Rev 94:1099–1142
10. Mulderry PK, Ghatei MA, Spokes RA, Jones PM, Pierson AM, Hamid QA, Kanse S, Amara SG, Burrin JM, Legon S et al (1988) Differential expression of alpha-CGRP and beta-CGRP by primary sensory neurons and enteric autonomic neurons of the rat. Neuroscience 25:195–205
11. Sternini C, Anderson K (1992) Calcitonin gene-related peptide-containing neurons supplying the rat digestive system: differential distribution and expression pattern. Somatosens Mot Res 9:45–59
12. Populin L, Stebbing MJ, Furness JB (2021) Neuronal regulation of the gut immune system and neuromodulation for treating inflammatory bowel disease. FASEB Bioadv 3:953–966
13. Tan KK, Brown MJ, Longmore J, Plumpton C, Hill RG (1994) Demonstration of the neurotransmitter role of calcitonin gene-related peptides (CGRP) by immunoblockade with anti-CGRP monoclonal antibodies. Br J Pharmacol 111:703–710
14. Russo AF, Hay DL (2023) CGRP physiology, pharmacology, and therapeutic targets: migraine and beyond. Physiol Rev 103:1565–1644
15. Rezaeian AH, Katafuchi T, Yoshizawa M, Hiraiwa N, Saito T, Nishibori M, Hamano K, Minamino N, Yasue H (2008) Genomic organization, expression and evolution of porcine CRSP1, 2, and 3. Cytogenet Genome Res 121:41–49
16. Schutz B, Mauer D, Salmon AM, Changeux JP, Zimmer A (2004) Analysis of the cellular expression pattern of beta-CGRP in alpha-CGRP-deficient mice. J Comp Neurol 476:32–43
17. Yang L, Xu M, Bhuiyan SA, Li J, Zhao J, Cohrs RJ, Susterich JT, Signorelli S, Green U, Stone JR et al (2022) Human and mouse trigeminal ganglia cell atlas implicates multiple cell types in migraine. Neuron 110:1806–1821 e1808
18. Barlowe CK, Miller EA (2013) Secretory protein biogenesis and traffic in the early secretory pathway. Genetics 193:383–410
19. Van den Berg B, Clemons WM Jr., Collinson I, Modis Y, Hartmann E, Harrison SC, Rapoport TA (2004) X-ray structure of a protein-conducting channel. Nature 427:36–44
20. Shennan KI, Taylor NA, Docherty K (1994) Calcium- and pH-dependent aggregation and membrane association of the precursor of the prohormone convertase PC2. J Biol Chem 269:18646–18650
21. Wu MM, Grabe M, Adams S, Tsien RY, Moore HP, Machen TE (2001) Mechanisms of pH regulation in the regulated secretory pathway. J Biol Chem 276:33027–33035
22. Chanat E, Huttner WB (1991) Milieu-induced, selective aggregation of regulated secretory proteins in the trans-golgi network. J Cell Biol 115:1505–1519
23. Yoo SH (1996) pH- and ca(2+)-dependent aggregation property of secretory vesicle matrix proteins and the potential role of chromogranins a and B in secretory vesicle biogenesis. J Biol Chem 271:1558–1565
24. Marzban L, Soukhatcheva G, Verchere CB (2005) Role of carboxypeptidase E in processing of pro-islet amyloid polypeptide in beta-cells. Endocrinology 146:1808–1817
25. Marzban L, Trigo-Gonzalez G, Verchere CB (2005) Processing of pro-islet amyloid polypeptide in the constitutive and regulated secretory pathways of beta cells. Mol Endocrinol 19:2154–2163
26. Carter ME, Soden ME, Zweifel LS, Palmiter RD (2013) Genetic identification of a neural circuit that suppresses appetite. Nature 503:111–114
27. Dux M, Vogler B, Kuhn A, Mackenzie KD, Stratton J, Messlinger K (2022) The Anti-CGRP antibody Fremanezumab lowers CGRP release from Rat Dura Mater and Meningeal Blood Flow. Cells.11
28. Reducha PV, Bomers JP, Edvinsson L, Haanes KA (2023) Rodent behavior following a dural inflammation model with anti-CGRP migraine medication treatment. Front Neurol 14:1082176
29. Melo-Carrillo A, Noseda R, Nir RR, Schain AJ, Stratton J, Strassman AM, Burstein R (2017) Selective inhibition of Trigeminovascular neurons by Fremanezumab: a humanized monoclonal Anti-CGRP antibody. J Neurosci 37:7149–7163
30. Kopruszinski CM, Turnes JM, Swiokla J, Weinstein TJ, Schwedt TJ, Dodick DW, Anderson T, Navratilova E, Porreca F (2021) CGRP monoclonal antibody prevents the loss of diffuse noxious inhibitory controls (DNIC) in a mouse model of post-traumatic headache. Cephalalgia 41:749–759
31. Jumper J, Evans R, Pritzel A, Green T, Figurnov M, Ronneberger O, Tunyasuvunakool K, Bates R, Zidek A, Potapenko A et al (2021) Highly accurate protein structure prediction with AlphaFold. Nature 596:583–589
32. Ma GQ, Wang B, Wang HB, Wang Q, Bao L (2008) Short elements with charged amino acids form clusters to sort protachykinin into large dense-core vesicles. Traffic 9:2165–2179
33. Mazzini G, Le Foll C, Boyle CN, Garelja ML, Zhyvoloup A, Miller MET, Hay DL, Raleigh DP, Lutz TA (2024) The processing intermediate of human amylin, pro-amylin(1–48), has in vivo and in vitro bioactivity. Biophys Chem 308:107201
34. Dhanvantari S, Loh YP (2000) Lipid raft association of carboxypeptidase E is necessary for its function as a regulated secretory pathway sorting receptor. J Biol Chem 275:29887–29893
35. Amara SG, Evans RM, Rosenfeld MG (1984) Calcitonin/calcitonin gene-related peptide transcription unit: tissue-specific expression involves selective use of alternative polyadenylation sites. Mol Cell Biol 4:2151–2160
36. Park HY, So SH, Lee WB, You SH, Yoo SH (2002) Purification, pH-dependent conformational change, aggregation, and secretory granule membrane binding property of secretogranin II (chromogranin C). Biochemistry 41:1259–1266
37. Dikeakos JD, Lacombe MJ, Mercure C, Mireuta M, Reudelhuber TL (2007) A hydrophobic patch in a charged alpha-helix is sufficient to target proteins to dense core secretory granules. J Biol Chem 282:1136–1143
38. Wu CB, Pan YM, Simizu Y (1995) Microsomal casein kinase II in endoplasmic reticulum- and golgi apparatus-rich fractions of ROS 17/2.8 osteoblast-like cells: an enzyme that modifies osteopontin. Calcif Tissue Int 57:285–292
39. Huang S, Wang Y (2017) Golgi structure formation, function, and post-translational modifications in mammalian cells. F1000Res.6:2050

Publisher's note